

---

<https://doi.org/10.15407/ujpe66.10.857>

V.A. NESTEROV, O.I. DAVYDOVSKA, V.YU. DENISOV

Institute for Nuclear Research, Nat. Acad. of Sci. of Ukraine  
(47, Nauky Ave., Kyiv 03028, Ukraine; e-mail: v.nest.v@gmail.com)

## SUBBARRIER-FUSION AND ELASTIC-SCATTERING CROSS-SECTIONS CALCULATED ON THE BASIS OF THE NUCLEUS-NUCLEUS POTENTIAL IN THE FRAMEWORK OF THE MODIFIED THOMAS-FERMI METHOD

---

*The nucleon density distributions and the nucleus-nucleus interaction potentials have been calculated for the  $^{16}\text{O} + ^{208}\text{Pb}$  and  $^{12}\text{C} + ^{208}\text{Pb}$  reactions using the modified Thomas-Fermi method, in which all terms up to  $\hbar^2$ -ones in the quasiclassical series expansion of the kinetic energy are taken into account. Skyrme forces depending on the nucleon density are used as the nucleon-nucleon interaction. On the basis of the obtained potentials, the cross-sections of subbarrier fusion and elastic scattering are calculated and agree well with the latest experimental data.*

*Keywords:* nucleus-nucleus interaction potential, modified Thomas-Fermi method, nucleon density distribution, cross-section, subbarrier fusion, elastic scattering.

### 1. Introduction

During the whole period of existence of theoretical nuclear physics, one of its main tasks consisted in finding out the regularities in the interaction between atomic nuclei. To calculate such fundamental characteristics of nuclear reactions as the cross-sections of various processes, we, first of all, need to know the potential energy of interaction between the nuclei [1–4]. Of particular importance is the information about the magnitude and radial dependence of the interaction potential at small distances between them.

Unfortunately, the potential of the nucleon-nucleon interaction, and even more so the nucleus-nucleus one, is currently unknown at length. In general, we can say that, qualitatively, it can be separated into the nuclear, Coulomb, and centrifugal parts, with the properties of the latter two components having

already been studied rather well. However, the situation with the nuclear part is much more complicated. Nowadays, a large number of various models are used for it [1–25], and the height of the barrier of the nucleus-nucleus interaction potential, which the reaction mechanism depends on, can differ substantially among those models. That is why the information concerning the potential of nucleus-nucleus interaction and the barrier height is extremely important for the description of the reaction process.

When building the potential of nucleus-nucleus interaction, considerably different methods are used [26–36]. In this work, a semimicroscopic approach was applied, in which the distribution of the nucleon density in nuclei and the distribution of their interaction energy density will be calculated in the framework of a modified Thomas-Fermi approach with concentration-dependent Skyrme forces [4, 7, 8, 10, 11, 13–17, 19–25]. At present, there are already a large number of successful parametrizations for the Skyrme interac-

---

© V.A. NESTEROV, O.I. DAVYDOVSKA,  
V.YU. DENISOV, 2021

tion. In this work, the SkM\* parametrization [32] is applied. In so doing, all possible terms up to  $\hbar^2$  in the series expansion of the quasiclassical distribution of the kinetic energy are taken into account. The calculations performed earlier by us and other authors for particular nuclear problems testify that the account of all gradient terms in the kinetic energy up to  $\hbar^2$  in the corresponding quasiclassical expansion is a rather accurate approximation, so we used it below. Under those conditions, the modified Thomas–Fermi approach with Skyrme forces can describe well the nucleon density distributions, the binding energy of nuclei, the root-mean-square nuclear radii, and many other characteristics of the ground and excited states of atomic nuclei [26–32, 34].

In our previous work [37], we constructed the potential of nucleus-nucleus interaction in the framework of the modified Thomas–Fermi method with Skyrme forces and calculated the subbarrier-fusion and elastic-scattering cross-sections for the  $^{16}\text{O} + ^{58,60,62,64}\text{Ni}$  systems. The results obtained demonstrate a good agreement with the experimental data. In this work, we extend this approach to the  $^{16}\text{O} + ^{208}\text{Pb}$  and  $^{12}\text{C} + ^{208}\text{Pb}$  systems: in the same manner, we calculate the potential of nucleus-nucleus interaction and, on this basis, obtain the subbarrier-fusion cross-sections and the angular distributions for the elastic scattering within the optical model.

In Section 2, the mathematical apparatus needed to implement the chosen approach is expounded. Sections 3 and 4 contain a discussion of the results obtained and our conclusions, respectively.

## 2. Modified Thomas–Fermi method

As was already mentioned, the potential of nucleus-nucleus interaction,  $V(R)$ , consists of the nuclear,  $V_N(R)$ , Coulomb  $V_{\text{COUL}}(R)$ , and centrifugal  $V_i(R)$ , components depending on the distance  $R$  between the centers of mass of the nuclei:

$$V(R) = V_N(R) + V_{\text{COUL}}(R) + V_i(R). \quad (1)$$

For the Coulomb and centrifugal parts, we use the well-known expressions, which can be found, in particular, in works [20, 23, 24]. The nuclear part of the interaction potential,  $V_N(R)$ , was calculated in the framework of a modified Thomas–Fermi method, in which all terms up to the second degree of  $\hbar$  in the quasiclassical series expansion of the kinetic energy

are taken into account [4, 7, 8, 10, 11, 13–25]. The density-dependent Skyrme forces – namely, the SkM\* parametrization [32] – were used as the nucleon-nucleon interaction. In this work, we apply the approximation of “frozen” nucleon densities, which is completely applicable to the case of near-barrier collision energies.

The potential of nucleus-nucleus interaction is defined as the difference between the energies of a system of two nuclei located at a finite distance  $R$ ,  $E_{12}(R)$ , and at the infinite distance from each other,  $E_1 + E_2$  [8, 10], i.e.

$$V(R) = E_{12}(R) - (E_1 + E_2), \quad (2)$$

$$E_{12} = \int \epsilon[\rho_{1p}(\mathbf{r}) + \rho_{2p}(\mathbf{r}, R), \rho_{1n}(\mathbf{r}) + \rho_{2n}(\mathbf{r}, R)] d\mathbf{r}. \quad (3)$$

The energy of the system at the infinite distance between the nucleons is the sum of the binding energies of separate nuclei,

$$E_{1(2)} = \int \epsilon[\rho_{1(2)p}(\mathbf{r}), \rho_{1(2)n}(\mathbf{r})] d\mathbf{r}. \quad (4)$$

Here,  $\rho_{1(2)n}$  and  $\rho_{1(2)p}$  are the neutron ( $n$ ) and proton ( $p$ ) densities in nucleus 1(2),  $\epsilon[\rho_{1(2)p}(\mathbf{r}), \rho_{1(2)n}(\mathbf{r})]$  is the energy density, and  $R$  is the distance between the centers of mass of the nuclei.

The energy density is the sum of the kinetic, potential, and Coulomb terms:

$$\epsilon = \epsilon_{\text{kin}} + \epsilon_{\text{pot}} + \epsilon_{\text{coul}}, \quad (5)$$

where  $\epsilon_{\text{kin}}$ ,  $\epsilon_{\text{pot}}$ , and  $\epsilon_{\text{coul}}$  denote the densities of the kinetic, potential, and Coulomb energies, respectively. If the density-dependent Skyrme forces are used, the specific formula for the energy density is well-known and was repeatedly cited in the literature [24–28, 30, 32, 37]. Therefore, since this formula is cumbersome, we do not present it here.

Let  $\tau$  denote the kinetic energy density, which is the sum of the kinetic energy densities for protons and neutrons,  $\tau = \tau_p + \tau_n$ . If the terms including up to the second degree of  $\hbar$  are retained in the quasiclassical expansion of the kinetic energy, we can write [7, 8, 10, 11, 24, 27, 28, 37] that

$$\tau = \tau_{\text{TF}} + \tau_2, \quad (6)$$

where  $\tau_{TF}$  is the kinetic energy of neutrons (protons) in the standard Thomas–Fermi approximation, and  $\tau_2$  is the  $\hbar^2$ -order gradient correction. The corresponding expressions are also rather cumbersome, and they can also be found in the literature [24, 25, 27, 28, 37]. Note that the contribution of the first term on the right-hand side of formula (6) dominates, but the gradient corrections also begin to play a significant role near the surface of the nucleus. Since the nucleus-nucleus potential at finite distances is associated with the interaction of nucleons in the overlap region of their density distribution “tails”, the account for gradient terms in the kinetic energy density and the realistic behavior of the nucleon density distribution in the diffuse region are very important while calculating the potential.

### 3. Calculations of the Nucleus-Nucleus Interaction Potential, and the Fusion and Elastic-Scattering Cross-Sections

To calculate the potential of nucleus-nucleus interaction, we have to know the distributions of nucleon densities in the interacting nuclei. In this work, we used the nucleon densities obtained in the framework of the modified Thomas–Fermi approach [4, 7, 8, 10, 11, 13–25] with Skyrme forces. In particular, the SkM\* parametrization [32] was applied to the latter. The nucleon density distributions for the  $^{12}\text{C}$ ,  $^{16}\text{O}$  and  $^{208}\text{Pb}$  nuclei, which were calculated using this method, are shown in Fig. 1.

Knowing the nucleon densities, we can write an expression for the energy density and proceed to the calculation of the nucleus-nucleus interaction potential. For this purpose, we can also apply the modified Thomas–Fermi approach with Skyrme forces (3)–(6). The resulting interaction potentials obtained by us for the  $^{16}\text{O} + ^{208}\text{Pb}$  and  $^{12}\text{C} + ^{208}\text{Pb}$  reactions are shown in Fig. 2.

From this figure, one can see that the calculated potentials of nucleus-nucleus interaction demonstrate a substantial repulsion at short distances. This repulsion results from the incompressibility of nuclear matter and the strong overlap of nucleon density distributions, because we calculated the interaction potential in the “frozen density” approximation. Such an overlap gives rise to the appearance of a region, where the nuclear matter density exceeds a value typical of the center of atomic nuclei, which is close to the density

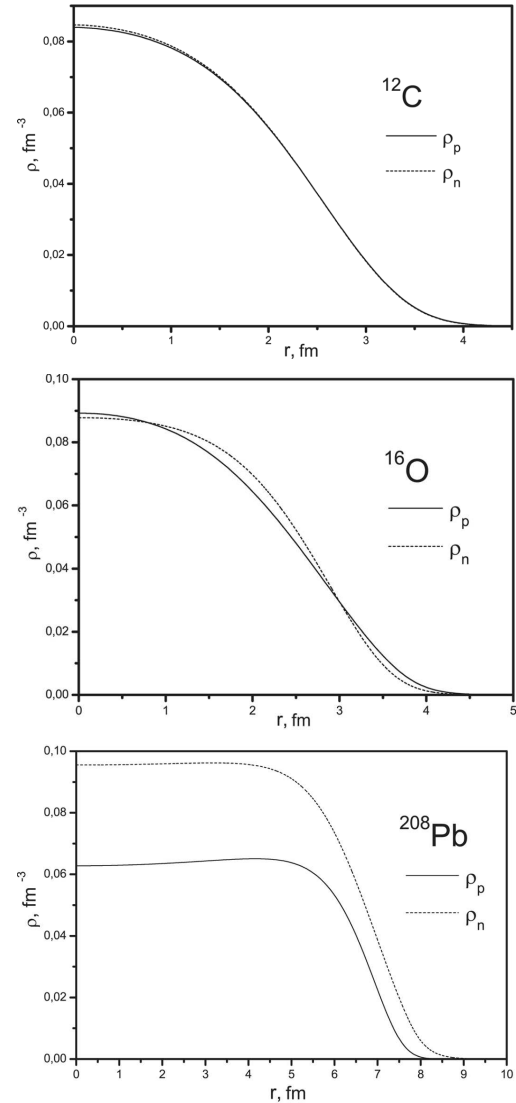


**Fig. 1.** Neutron and proton densities in the  $^{12}\text{C}$ ,  $^{16}\text{O}$ , and  $^{208}\text{Pb}$  nuclei calculated in the framework of the modified Thomas–Fermi approach

of nuclear matter. The presence of a pronounced repulsion core associated with both the strong overlap of the nucleon density distributions and a low value of the compression modulus for nuclear matter also leads to their relaxation.

On the basis of obtained potentials, we can pass to direct calculations of the cross-sections of nuclear reactions. First of all, we parametrize the nuclear parts of the nucleus-nucleus interaction potentials using the Woods–Saxon potential [1–4], because most of the

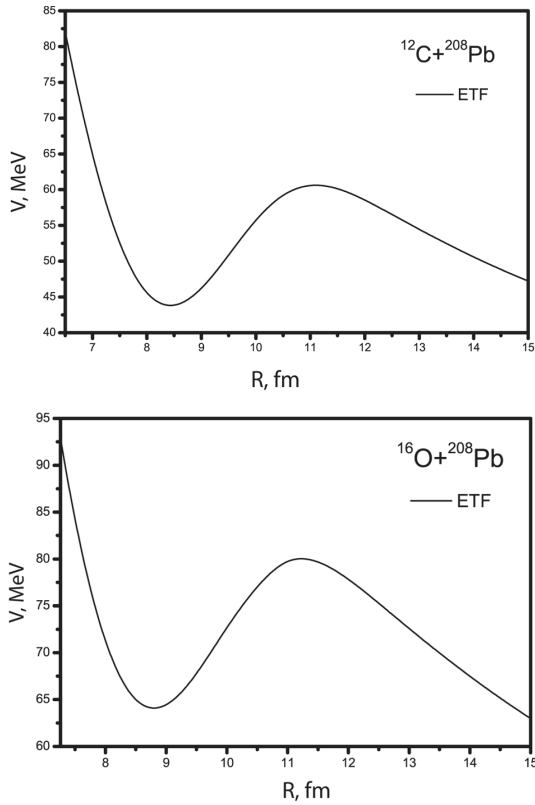


**Fig. 2.** Nucleus-nucleus interaction potentials calculated in the framework of the modified Thomas–Fermi approach for the  $^{16}\text{O} + ^{208}\text{Pb}$  and  $^{12}\text{C} + ^{208}\text{Pb}$  systems

known codes for the calculation of the cross-sections of nuclear reactions take the interaction potential into account just in this form:

$$V_{\text{WS}}(R) = \frac{-V_0}{1 + \exp \frac{R-r_0(A_1^{1/3} + A_2^{1/3})}{d_0}}. \quad (7)$$

The main attention was focused on the quality of the parametrization in a vicinity of the contact point of the nuclei, because this region is the most important for describing both the elastic scattering and subbarrier fusion phenomena.

**Table 1. Parameters of the Woods–Saxon potential (7) used to approximate the nuclear parts of the interaction potentials obtained in the framework of the modified Thomas–Fermi approach**

Reaction	$V_0$ , MeV	$r_0$ , fm	$d_0$ , fm
$^{12}\text{C} + ^{208}\text{Pb}$	55.4837	1.1363	0.6591
$^{16}\text{O} + ^{208}\text{Pb}$	66.1147	1.1333	0.7421

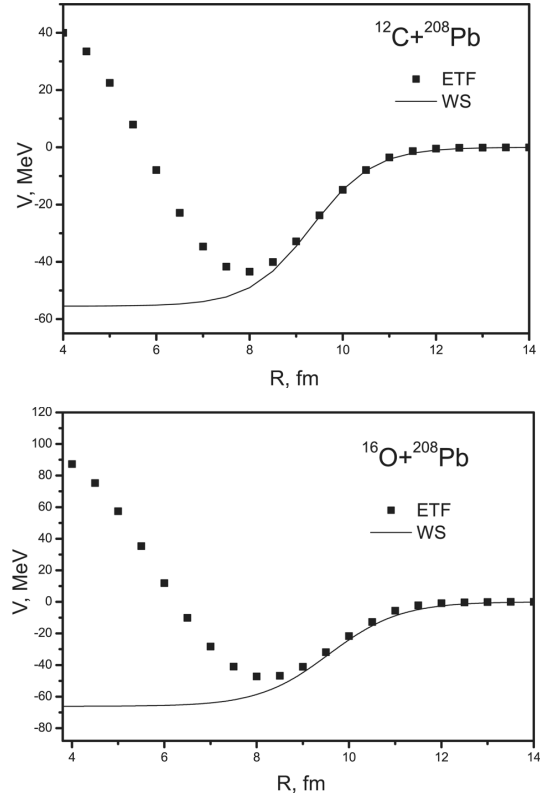


**Fig. 3.** Woods–Saxon potentials used to approximate the nuclear parts of the interaction potentials obtained in the framework of the modified Thomas–Fermi approach

rier fusion phenomena. The values of the parameters of the Woods–Saxon potential (7) calculated for the  $^{16}\text{O} + ^{208}\text{Pb}$  and  $^{12}\text{C} + ^{208}\text{Pb}$  systems are quoted in Table 1. In addition, in Fig. 3, one can see the nuclear parts of the interaction potentials and their approximations using the Woods–Saxon potential. It is evident that the obtained Woods–Saxon potentials describe well the nuclear part of the interaction at the distances when the nuclei begin to contact each other. As was already mentioned, this interval of distances is especially important for describing nuclear processes at energies close to the barrier ones.

In order to calculate the cross-sections of subbarrier fusion, we used the well-known CCFULL program code [38], which involves the coupling of reaction channels with low-lying multipole vibrational surface excitations  $2^+$  and  $3^-$  in the interacting nuclei. The CCFULL code also includes the nonlinear effects of the coupling with multiphonon multipole surface excitations. The parameters for the quadrupole and oc-

tupole deformations and the excitation energy of low-energy vibrational  $2^+$  and  $3^-$  states (see Table 2) were taken from the corresponding tables in works [39–41].

The subbarrier-fusion cross-sections obtained for the  $^{12}\text{C} + ^{208}\text{Pb}$  and  $^{16}\text{O} + ^{208}\text{Pb}$  systems using the CCFULL program code [38] are shown in Figs. 4 and 5, respectively. As one can see, the calculated cross-sections of the subbarrier fusion describe well the latest experimental data for those reactions, which were taken from works [42–44].

For the  $^{12}\text{C} + ^{208}\text{Pb}$  and  $^{16}\text{O} + ^{208}\text{Pb}$  systems, we also calculated the elastic-scattering cross-sections in the framework of the optical model using the obtained nuclear components of the potentials as the real parts of the interaction. Our calculations in the optical model took only the elastic channel into account and did not consider the coupling with low-energy surface vibrational states. In calculations, the imaginary part was added to the obtained nuclear potential in the form of the sum of the bulk and surface terms:

$$W(R) = -\frac{W_W}{1 + \exp[R - r_W(A_1^{1/3} + A_2^{1/3})/d_W]} - \frac{W_S \exp[R - r_S(A_1^{1/3} + A_2^{1/3})/d_S]}{d_S(1 + \exp[R - r_S(A_1^{1/3} + A_2^{1/3})/d_S])}. \quad (8)$$

**Table 2. Parameters of quadrupole and octupole deformations and excitation energies of low-energy vibrational states  $2^+$  and  $3^-$  [39–41]**

Nucleus	$\beta_2$	$E_x(2_1^+)$ , keV	$\beta_3$	$E_x(3_1^-)$ , keV
$^{12}\text{C}$	0.582	4438.9	0.832	9641
$^{16}\text{O}$	0.349	6917.1	0.729	6130
$^{208}\text{Pb}$	0.0553	4085.5	0.111	2615

**Table 3. Parameters of the imaginary part of the nuclear potential obtained by fitting the experimental elastic-scattering cross-sections using the Woods–Saxon potential, which approximates the nucleus-nucleus potential in the modified Thomas–Fermi method, for the  $^{16}\text{O} + ^{208}\text{Pb}$  and  $^{12}\text{C} + ^{208}\text{Pb}$  reactions**

Reaction	$W_W$	$r_W$	$d_W$	$W_S$	$r_S$	$d_S$
$^{16}\text{O} + ^{208}\text{Pb}$	20.205	1.100	0.516	14.999	1.299	0.553
$^{12}\text{C} + ^{208}\text{Pb}$	19.000	1.265	0.699	13.397	1.286	0.633

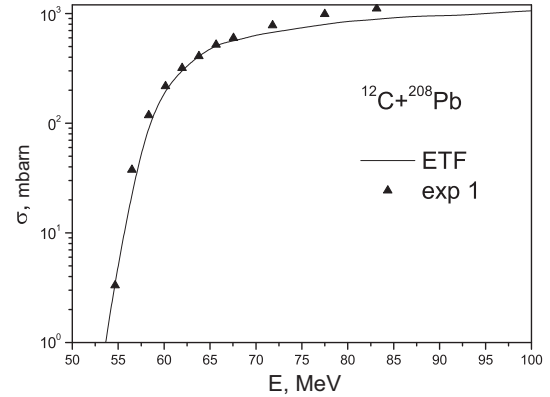


**Fig. 4.** Subbarrier-fusion cross-section for the  $^{12}\text{C} + ^{208}\text{Pb}$  system obtained on the basis of the interaction potential in the framework of the modified Thomas–Fermi approach. Experimental data were taken from work [42]

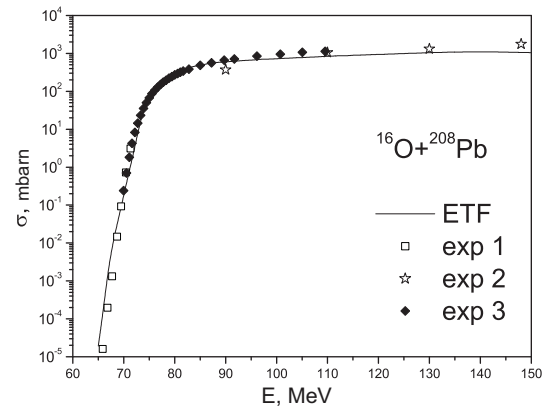


**Fig. 5.** Subbarrier-fusion cross-section for the  $^{16}\text{O} + ^{208}\text{Pb}$  system obtained on the basis of the interaction potential in the framework of the modified Thomas–Fermi approach. Experimental data were taken from works [43, 44]

Here, the parameters  $W_W$ ,  $r_W$ ,  $d_W$ ,  $W_S$ ,  $r_S$ , and  $d_S$  are the force, radius, and diffusivity, respectively, of the bulk ( $W$ ) and surface ( $S$ ) parts of the imaginary nuclear potential. Just this expression is used, as a rule, in the theory of nuclear collisions [2, 4, 36]. The parameters of the imaginary part of the nuclear potential (see Table 3) were found by fitting the experimental elastic-scattering cross-section making use of the Woods–Saxon potential (7), which approximates the nucleus-nucleus potential obtained by the modified Thomas–Fermi method (Table 1).

The results of calculations of the elastic-scattering cross-sections for the  $^{16}\text{O} + ^{208}\text{Pb}$  system at the beam energy  $E_{\text{lab}} = 95$  MeV and the  $^{12}\text{C} + ^{208}\text{Pb}$  sys-

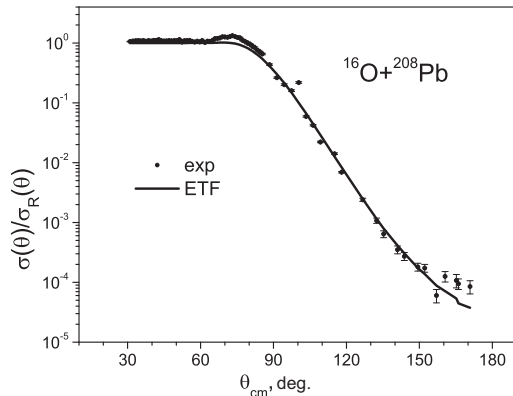


**Fig. 6.** Elastic-scattering cross-section for the  $^{16}\text{O} + ^{208}\text{Pb}$  system obtained on the basis of the interaction potential of the modified Thomas–Fermi approach with density-dependent Skyrme forces. The beam energy  $E_{\text{lab}} = 95$  MeV. Experimental data were taken from work [45]

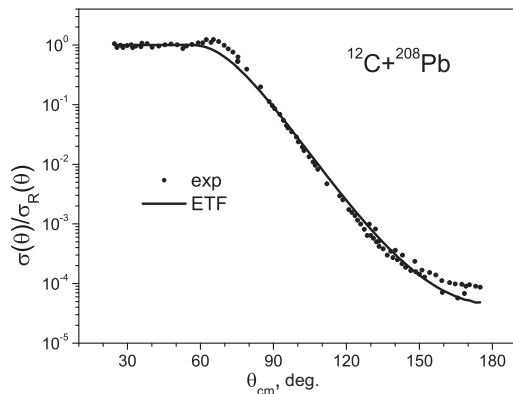


**Fig. 7.** Elastic-scattering cross-section for the  $^{12}\text{C} + ^{208}\text{Pb}$  system obtained on the basis of the interaction potential of the modified Thomas–Fermi approach with density-dependent Skyrme forces. The beam energy  $E_{\text{lab}} = 75.7$  MeV. Experimental data were taken from work [45]

tem at the beam energy  $E_{\text{lab}} = 75.7$  MeV are illustrated in Figs. 6 and 7, respectively, where the elastic-scattering cross-section values are normalized to the Rutherford cross-section. The experimental data shown in the figures were taken from work [45]. As we can see from those figures, the calculated elastic-scattering cross-sections agree well with the corresponding experimental data.

#### 4. Conclusions

In this work, we have calculated the nucleus-nucleus interaction potentials for the  $^{16}\text{O} + ^{208}\text{Pb}$  and

$^{12}\text{C} + ^{208}\text{Pb}$  reactions in the framework of the modified Thomas–Fermi approach with density-dependent Skyrme forces using the nucleon densities obtained within the same approach. The potentials were calculated in the “frozen density” approximation, which is quite applicable at the collision energies close to the barrier ones. This approximation allowed us to analyze the properties of nucleus-nucleus interaction in a vicinity of the contact point of the nuclei in detail. On the basis of the obtained potentials, we have calculated the subbarrier-fusion and elastic-scattering cross-sections for the  $^{16}\text{O} + ^{208}\text{Pb}$  and  $^{12}\text{C} + ^{208}\text{Pb}$  systems. The obtained cross-sections of these processes are found to be in good agreement with the latest experimental data. Note that the application of a single potential made it possible to simultaneously describe the experimental cross-sections of both subbarrier fusion and elastic scattering.

1. R. Bass. *Nuclear Reactions with Heavy Ion* (Springer, 1980) [ISBN: 978-3-540-09611-5].
2. G.R. Satchler. *Direct Nuclear Reactions* (Clarendon Press, 1983) [ISBN-13: 978-0198512691, ISBN-10: 0198512694].
3. P. Frobrich, R. Lipperheide. *Theory of Nuclear Reactions* (Clarendon Press, 1996) [ISBN: 9780198537830].
4. V.Yu. Denisov, V.A. Plyuiko. *Problems of the Physics of Atomic Nucleus and Nuclear Reactions* (Kyiv University, 2013) (in Russian).
5. J. Blocki, J.Randrup, W.J. Swiatecki, C.F.Tsang. Proximity forces. *Ann. Phys.* **105**, 427 (1977).
6. W.D. Myers and W.J. Swiatecki. Nucleus-nucleus proximity potential and superheavy nuclei. *Phys. Rev. C* **62**, 044610 (2000).
7. V.Yu. Denisov and V.A. Nesterov. Potential of interaction between nuclei and nucleon-density distribution in nuclei. *Phys. Atom. Nucl.* **69**, 1472 (2006).
8. V.Yu. Denisov. Interaction potential between heavy ions. *Phys. Lett. B* **526**, 315 (2002).
9. H.J. Krappe, J.R. Nix, A.J. Sierk. Unified nuclear potential for heavy-ion elastic scattering, fusion, fission, and ground-state masses and deformations. *Phys. Rev. C* **20**, 992 (1979).
10. V.Yu. Denisov, W. Norenberg. Entrance channel potentials in the synthesis of the heaviest nuclei. *Eur. Phys. J. A* **15**, 375 (2002).
11. V.Yu. Denisov. Nucleus-nucleus potential with shell-correction contribution. *Phys. Rev. C* **91**, 024603 (2015).
12. A. Winther. Dissipation, polarization and fluctuation in grazing heavy-ion collisions and the boundary to the chaotic regime. *Nucl. Phys. A* **594**, 203 (1995).
13. V.Yu. Denisov, O.I. Davidovskaya. Repulsive core potential and elastic heavy-ion collisions. *Yad. Fiz.* **73**, 429 (2010).

14. V.Yu. Denisov, O.I. Davidovskaya. Repulsive core potential and elastic heavy-ion collisions. *Ukr. J. Phys.* **54**, 669 (2009).
15. K.A. Brueckner, J.R. Buchler, M.M. Kelly. New theoretical approach to nuclear heavy-ion scattering. *Phys. Rev. C* **173**, 944 (1968).
16. J. Fleckner, U. Mosel. Antisymmetrization effects in heavy ion potentials. *Nucl. Phys. A* **277**, 170 (1977).
17. O.I. Davidovskaya, V.Yu. Denisov, V.A. Nesterov. Nucleus-nucleus potential with repulsive core and elastic scattering. Part 1. Nucleus-nucleus interaction potential. *Yad. Fiz. Energ.* **11**, No. 1, 25 (2010).
18. O.I. Davidovskaya, V.Yu. Denisov, V.A. Nesterov. Nucleus-nucleus potential with repulsive core and elastic scattering. Part 2. The elastic scattering cross sections with and without core. *Yad. Fiz. Energ.* **11**, No. 1, 33 (2010).
19. V.Yu. Denisov, O.I. Davidovskaya. Elastic scattering of heavy ions and the nucleus-nucleus potential with a repulsive core. *Izv. Ross. Akad. Nauk Ser. Phys.* **74**, 611 (2010) (in Russian).
20. O.I. Davidovskaya, V.Yu. Denisov, V.A. Nesterov. Effective nucleus-nucleus potential with the contribution of the kinetic energy of nucleons, and the cross-sections of elastic scattering and subbarrier fusion. *Ukr. J. Phys.* **62**, 473 (2017).
21. V.A. Nesterov. Effect of the Pauli exclusion principle and the polarization of nuclei on the potential of their interaction for the example of the  $^{16}\text{O} + ^{16}\text{O}$  system. *Phys. At. Nucl.* **76**, 577 (2013).
22. V.Yu. Denisov, O.I. Davidovskaya. Elastic  $^{16}\text{O} + ^{16}\text{O}$  scattering and nucleus-nucleus potential with a repulsive core. *Ukr. J. Phys.* **55**, 861 (2010).
23. O.I. Davidovskaya, V.Yu. Denisov, V.O. Nesterov. Nucleus-nucleus potential, elastic-scattering and subbarrier-fusion cross-sections for the  $^{40}\text{Ca} + ^{40}\text{Ca}$  system. *Yad. Fiz. Energ.* **19**, 203 (2018) (in Ukrainian).
24. O.I. Davydovska, V.Yu. Denisov, V.A. Nesterov. Comparison of the nucleus-nucleus potential evaluated in the double-folding and energy density approximations and the cross-sections of elastic scattering and fusion of heavy ions. *Nucl. Phys. A* **989**, 214 (2019).
25. V.O. Nesterov, O.I. Davydovska, V.Yu. Denisov. Calculations of the subbarrier-fusion and elastic-scattering cross-sections for heavy ions using the modified Thomas–Fermi potential with Skyrme forces. *Yad. Fiz. Energ.* **20**, 349 (2019) (in Ukrainian).
26. P. Ring, P. Schuck. *The Nuclear Many-Body Problem* (Springer-Verlag, 1980) [ISBN: 978-3-540-21206-5].
27. M. Brack, C. Guet, H.B. Hakanson. Self-consistent semiclassical description of average nuclear properties – a link between microscopic and macroscopic models. *Phys. Rep.* **123**, 275 (1985).
28. M. Brack, R.K. Bhaduri, *Semiclassical Physics* (Addison-Wesley, 1997) [ISBN-10: 0813340845; ISBN-13: 978-0813340845].
29. V.M. Strutinsky, A.G. Magner, V.Yu. Denisov. Density distributions in nuclei. *Z. Phys. A* **322**, 149 (1985).
30. J. Dobaczewski, W. Nazarewicz, P.G. Reinhard. Pairing interaction and self-consistent densities in neutron-rich nuclei. *Nucl. Phys. A* **693**, 361 (2001).
31. D. Vautherin, D.M. Brink. Hartree-Fock calculations with Skyrme’s interaction. I. Spherical nuclei. *Phys. Rev. C* **5**, 626 (1972).
32. J. Bartel, P. Quentin, M. Brack, C. Guet, H.B. Håkansson. Towards a better parametrisation of Skyrme-like effective forces: A critical study of the SkM force. *Nucl. Phys. A* **386**, 79 (1982).
33. S.A. Fayans, S.V. Tolokonnikov, E.L. Trykov, D. Zawischac. Nuclear isotope shifts within the local energy-density functional approach. *Nucl. Phys. A* **676**, 49 (2000).
34. J.W. Negele. The mean-field theory of nuclear structure and dynamics. *Rev. Mod. Phys.* **54**, 913 (1982).
35. T.H.R. Skyrme. The effective nuclear potential. *Nucl. Phys.* **9**, 615 (1959).
36. H. Feshbach. The optical model and its justification. *Annu. Rev. Nucl. Sci.* **8**, 49 (1958).
37. O.I. Davydovska, V.A. Nesterov, V.Yu. Denisov. The nucleus-nucleus potential within the extended Thomas–Fermi method and the cross-sections of subbarrier fusion and elastic scattering for the systems  $^{16}\text{O} + ^{58,60,62,64}\text{Ni}$ . *Nucl. Phys. A* **1002**, 121994 (2020).
38. K. Hagino, N. Rowley, A.T. Kruppa. A program for coupled-channel calculations with all order couplings for heavy-ion fusion reactions. *Comput. Phys. Commun.* **123**, 143 (1999).
39. B. Pritychenko, M. Birch, B. Singh, M. Horoi. Tables of E2 transition probabilities from the first  $2^+$  image states in even–even nuclei. *At. Data Nucl. Data Tabl.* **107**, 1 (2016).
40. T. Kibedi, R.H. Spear. Reduced electric-octupole transition probabilities,  $B(E3; 0_1^+ \rightarrow 3_1^-)$  – an update. *At. Data Nucl. Data Tabl.* **80**, 35 (2002).
41. S. Raman, C.W. Nestor, P. Tikkanen. Transition probability from the ground to the first excited  $2^+$  state of even-even nuclei. *At. Data Nucl. Data Tabl.* **78**, 1 (2001).
42. A. Mukherjee, D.J. Hinde, M. Dasgupta, K. Hagino, J.O. Newton, R.D. Butt. Failure of the Woods–Saxon nuclear potential to simultaneously reproduce precise fusion and elastic scattering measurements. *Phys. Rev. C* **75**, 044608 (2007).
43. C.R. Morton, A.C. Berriman, M. Dasgupta, D.J. Hinde, J.O. Newton, K. Hagino, I.J. Thompson. Coupled-channels analysis of the  $^{16}\text{O} + ^{208}\text{Pb}$  fusion barrier distribution. *Phys. Rev. C* **60**, 044608 (1999).
44. M. Dasgupta, D.J. Hinde, A. Diaz-Torres, B. Bouriquet, C.I. Low, G.J. Milburn, J.O. Newton. Beyond the coherent coupled channels description of nuclear fusion. *Phys. Rev. Lett.* **99**, 192701 (2007).

45. V.P. Rudakov, K.P. Artemov, Yu.A. Glukhov, S.A. Goncharov, A.S. Demyanova, A.A. Ogloblin, V.V. Paramonov, M.V. Rozhkov. Elastic  $^{12}\text{C} + ^{208}\text{Pb}$  and  $^{16}\text{O} + ^{208}\text{Pb}$  scattering and the form of the potential barrier. *Bull. Russ. Acad. Sci. Phys.* **65**, 57 (2001).

Received 04.03.21.

Translated from Ukrainian by O.I. Voitenko

*В.О. Нестеров, О.І. Давидовська, В.Ю. Денисов*

ПОПЕРЕЧНІ ПЕРЕРІЗИ ПІДБАР'ЄРНОГО  
ЗЛИТТЯ ТА ПРУЖНОГО РОЗСІЯННЯ, ОДЕРЖАНІ  
НА ОСНОВІ МІЖЯДЕРНОГО ПОТЕНЦІАЛУ  
В МОДИФІКОВАНОМУ МЕТОДІ ТОМАСА–ФЕРМІ

Густини розподілу нуклонів та потенціали міжядерної взаємодії для реакцій  $^{16}\text{O} + ^{208}\text{Pb}$  та  $^{12}\text{C} + ^{208}\text{Pb}$  було розра-

ховано в рамках модифікованого методу Томаса–Фермі, з урахуванням усіх доданків до членів другого порядку по  $\hbar$  у квазікласичному розкладі кінетичної енергії. В ролі нуклон-нуклонної взаємодії використовувалися сили Скірма, залежні від густини нуклонів. На основі одержаних потенціалів були обчислені перерізи підбар'єрного злиття та пружного розсіяння, що добре узгоджуються з новітніми експериментальними даними.

*Ключові слова:* потенціал міжядерної взаємодії, модифікований метод Томаса–Фермі, розподіл густини нуклонів, поперечний переріз, підбар'єрне злиття, пружне розсіяння.